Applied Surface Science 256 (2010) 6506–6511

Contents lists available at ScienceDirect

Applied Surface Science

journal homepage: www.elsevier.com/locate/apsusc

Structure evolution from nanocolumns to nanoporous of nitrogen doped amorphous carbon films deposited by magnetron sputtering

Bin Zhang[a,b], Yuanlie Yu[a,b], Zhou Wang[a,b], Junyan Zhang[a,*]

[a] State Key Laboratory of Solid Lubrication, Lanzhou Institute of Chemical Physics, Chinese Academy of Sciences, Lanzhou 730000, China
[b] Graduate School of the Chinese Academy of Sciences, Beijing 100039, China

ARTICLE INFO

Article history:
Received 21 January 2010
Received in revised form 1 April 2010
Accepted 1 April 2010
Available online 8 April 2010

Keywords:
Nanocolumn structure
Nanoporous structure
Field emission properties

ABSTRACT

Different nitrogen doped amorphous carbon (CNx) films were obtained by magnetron sputtering of carbon target in argon and nitrogen atmosphere at the increasing negative bias voltages from 0 to 150 V. The films structures have experienced great change, from the novel column to nanoporous structure at the bias voltage of 0 V to the porous structure at 150 V. The proposed growth process was that the CNx nuclei grew at 0 V acted as the "seeds" for the growth of the nanocolumns, and ion etching effects at 150 V induced the formation of nanoporous structures. Furthermore, a comparison study showed that the field emission properties of the CNx films were related with the introduction of the nitrogen atoms, the size and concentration of sp^2 C clusters and the surface roughness. The films with rougher surface have lower threshold field.

1. Introduction

Carbon-based nanostructure materials, possessing excellent mechanical, chemical, optic and electronic properties, have received great attention in the past decades. Many techniques, e.g. plasma enhanced chemical vapor deposition (PECVD) [1], low-energy cluster beam deposition (LECBD) [2], glancing angle deposition (GLAD) [3], focused ion beam (FIB) [4], and arc discharge [5], were employed to fabricate new kinds of carbon-based nanostructure materials. These nanostructures with controlled structures and dimensions, such as nanotubes, nanoparticles, nanowires, nanoporous, nanolayers and nanocolumns [1–8], have great potential applications in various nano/microelectromechanical, emitters in advanced field emission devices, adsorbents for bulky pollutants, and as electrodes for supercapacitors [1–10].

Currently, nitrogen are widely used as n-type dopant that can effectively manipulate the films microstructure and modify the carbon-based films properties, because nitrogen doping particularly cause the reduction of the energy barrier of the curvature in the basal planes by creating pentagons or heptagons to form nanostructures at lower temperatures. With the presence of nitrogen, fullerene-like carbon nitride films, bamboo-like carbon nanotubes (CNTs) and carbon nitride (CNx) nanocolumns were successfully prepared by radio frequency magnetron sputtering [10–13]. Moreover, some researchers have carefully investigated the influence of nitrogen content on the growth and structures of CNx films [14–16], indicating that their microstructures, morphologies and properties were greatly dependent on the growth parameters [14–16].

Scalese et al. [12] firstly reported that the fabrication of CNx nanocolumns on silicon wafers was performed by radio-frequency magnetron sputtering at high temperature of 400–600 °C. In our previous work, the CNx nanocolumns were successfully fabricated at the low temperature with the assistance of the nickel catalyst [11]. However, the influence of the negative bias voltage on the structure evolution of CNx nanocolumns was rarely mentioned and not systematically investigated. Therefore, we focused on the investigation of the microstructure evolution of the CNx film at different negative bias. Additionally, the field emission performance was also discussed.

2. Experimental details

Nanostructured CNx films has been fabricated on the N(1 0 0) silicon substrates using a 20 kHz dual target middle frequency magnetron sputtering with a specific power of about 0.065 W/cm^2 (target size: 25 mm × 8 mm × 5 mm) at 300 °C. A resistively heated substrate holder with a distance of 140 mm was placed parallel to carbon target. More details of the deposition system are given elsewhere [11]. The substrates were chemically and ultrasonically cleaned before their introduction into the deposition chamber. Prior to deposition, a base pressure of 4.0×10^{-3} Pa was achieved

* Corresponding author. Tel.: +86 931 4968295; fax: +86 931 4968295.
E-mail address: zhangjunyan@lzb.ac.cn (J. Zhang).

0169-4332/$ – see front matter © 2010 Elsevier B.V. All rights reserved.
doi:10.1016/j.apsusc.2010.04.002

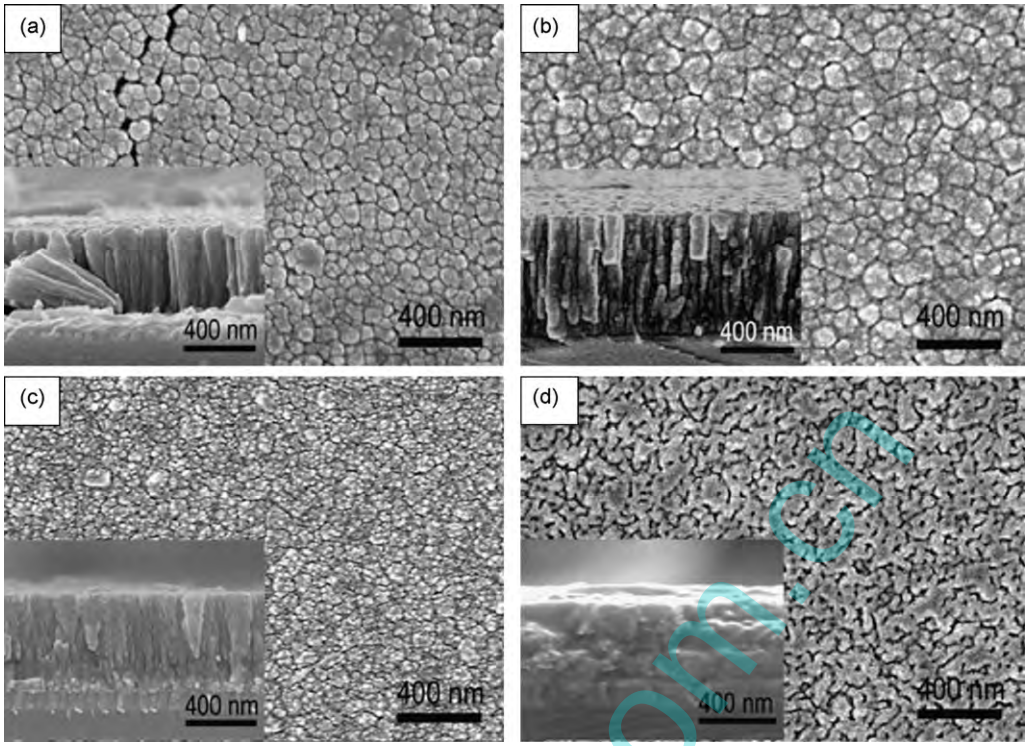

Fig. 1. FE-SEM images of surface and cross-section of the CNx films deposited on Si under 0.5 Pa with a fixed N_2/Ar ratio (2:5) at different substrates bias: for the film deposited at 0 V (a) for the film deposited −50 V (b) for the film deposited −100 V (c) for the film deposited −150 V (d).

in the chamber with a turbomolecular pumping system. The films were deposited with a pyrolytic carbon target (99.99%) as carbon source. A mixture of 150 sccm nitrogen and 60 sccm argon was introduced in the chamber as reactive gas. In all experiments, once the temperature reached 300 °C, the mixture gases were fed into the vacuum chamber to 0.5 Pa and the deposition was initiated. Depending on self-bias modulated from 0 to 150 V, a series of nanostructured CNx films, from nanocolumns to cluster assembled CNx films with worm-like porous morphology, were obtained after 100 min.

The thicknesses of the films were measured by a surface profilometer, from the step formed at the edge of the coating due to the substrate clamping. A JSM-6701F field emission scanning electron microscopy (FE-SEM) was employed to examine the morphologies of the as-deposited films. Raman spectra of all samples were measured by a micro-Raman with a LABRAM HR 800 microspectrometer at wavelength of 532 nm (2.3 eV). The chemical component of the films was determined by a PHI-5702 multifunctional X-ray photoelectron spectroscopy (XPS), Al Kα radiation (photo energy 1486.6 eV) as the excitation source. The energy analyzer energy was set such that the Au ($4f_{7/2}$) line was recorded with a full width at half maximum of 0.9 eV. Fourier transform infrared (FTIR) spectra of CNx films were recorded on an IFS66V/S spectrometer to detect the changes of the bonding structure in the films. The morphologies of the as-deposited films were observed by CSPM4000 atomic force microscopy (AFM), using "constant-force" mode and a Si_3N_4 tip.

Field emission properties of the resulted films as a cathode were tested by a field emission device in a vacuum of 1.0×10^{-4} Pa. A cylindrical nickel chrome rod with the diameter of 8 mm was used as anode, with a distance between the cathodes was set at 50 μm and the testing cathode area was 0.5 cm × 0.5 cm, whereas the as-deposited samples serving as cathode. During testing process, a brass plate pressed on the edge of the sample surface assures the electrical contact.

3. Results and discussion

3.1. FE-SEM images

The FE-SEM images of the surface and cross-section of the CNx films deposited at different negative bias are given in Fig. 1. The film prepared without negative bias, showed an arrayed nanocolumn structure with dome-like surface (Fig. 1a). In the cases of the negative bias at 50 and 100 V (Fig. 1b and c), the columnar structure gradually weakened. And the columnar structure completely disappeared and a worm-like porous appeared at higher value of the negative bias (150 V) (Fig. 1d), which might be related with the bombardment effect of high-energy N ions at 150 V. Detailed explanation will be given below.

3.2. Chemical composition and bonding states

The chemical composition and bonding states of the as-deposited films were determined by XPS. As shown in Fig. 2, clearly, the nitrogen content and the deposition rate were strongly related with the variation of the negative bias. When the negative bias reached to 50 V, the nitrogen content came to the maximum values (15.3 ± 0.4%) as well as the deposition rate (6.8 ± 0.2 nm/min). That was in good accordance with those reported by Inoue et al. [13] and Ling et al. [14]. They proposed that nitrogen ions bombardment induced by the negative bias played an important role in CNx film growth. At the lower negative bias, the bombardment with a low-energy particles stream could effectively enhance surface mobility and consequently facilitate film growth. At the excessively higher negative bias, ion bombardment with higher energy particles probably resulted in the chemical and physical etching process, which greatly affected the kinetics of C–N reaction and limited nitrogen content and lowed deposition rate in CNx film [13–15]. The preferential desorption of volatile N_2 and CN-species, should be responsible for the reduction of nitrogen content when the fabrica-

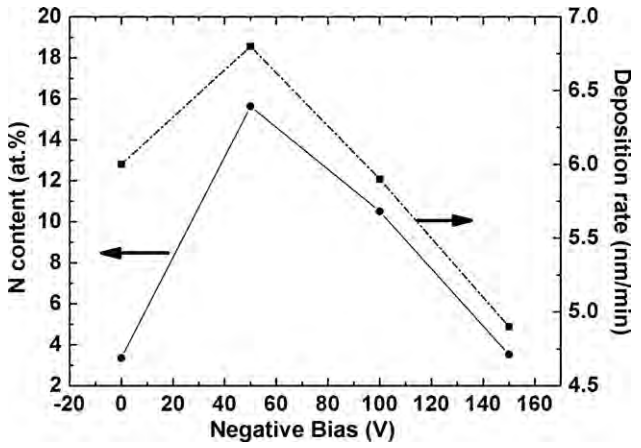

Fig. 2. N atoms content (at.%) and deposition rate plot as bias function.

tion of CNx film was performed at higher bias voltage. Particularly, bonds in the interface of the disturbance particles were probably unstable, and could be easily broken out by high-energy particles bombardment, giving rise to a porous structure.

In order to get quantitative information on the chemical composition and bonding states of the as-deposited films, the C1s spectra of the prepared films were fitted by the method already described in a previous paper [16–19] (Fig. 3). The first component C1, denoted as for pure carbon, may be located at 284.4 eV (C1). The second one C2 around 285.2 eV can be attributed to aromatic CN structures with three C atoms bonded to one N atom. The third one C3 located at 286.3 eV can be ascribed to non-aromatic CN phase including sp^3 C bonded to N. The forth component C4 around 287.9 eV (C4) can be assigned to non-aromatic CN bonds with C atoms having two neighboring N atoms, and a fifth component C5 around 288.8 eV can be assigned to C=O bonding types, respectively [16–19]. The results are shown in Fig. 3.

Table 1
XPS C1s fitting results of the CNx films deposited at different negative bias.

Samples	C1	C2	C3	C4	C5
0 V	75.0	9.5	9.4	4.5	1.6
50 V	41.0	28.2	20.2	6.7	3.9
100 V	42.1	29.6	17.8	6.9	3.6
150 V	55.5	26.0	12.0	4.0	2.5

The results on the C bonding state evolution as the function of the applied negative bias could give more detailed information, summarized in Table 1. [C1] fraction of C sp^2 decreased suddenly to 41% at the negative bias of 50 V, and gradually increased with the increasing of the negative bias to about 55.5%. [C2] fraction of C sp^2 increased abruptly to 28.2% at the negative bias of 50 V and did not greatly change with the increasing negative bias. The fraction [C3 + C4] increased to 26.9% at the negative bias of 50 V, and decreased to 16% at the negative bias of 150 V. The changes of C5 resembled with that of [C3 + C4].

The N1s spectra of the prepared films were also deconvoluted, as shown in Fig. 4. According to the previous work [16–19], peak N1 (398.2 ± 0.2 eV) is related to non-aromatic CN bonds with N having either a sp^3 hybridization or N bonded to sp^3 carbon (NC_3). Peak N2 (399.2 ± 0.2 eV) can be attributed to N atoms in pyridine structure (aromatic NC_2). Peak N3, located around 400.7 ± 0.2 eV is characteristic of sp^2 CN structures where N substitutes for C in extended aromatic structures (aromatic NC_3). Peak N4 (402.3 ± 0.6 eV) can be associated to N–O groups. The results of this analysis are summarized in Table 2.

With the increasing of the applied negative bias, the N1 fraction decreased to 35% at the negative bias of 50 V and gradually increased to 43.4%, which was different from the N2, N3 and N4 fractions variations. The fraction [N2 + N3], related to the aromatic domains, firstly increased when the applied negative bias increased from 0 to 50 V, but decreased gradually with the increasing of the applied negative bias. The N4 fraction showed the maximum value (16.7%) at 150 V. This is a pointer that porous struc-

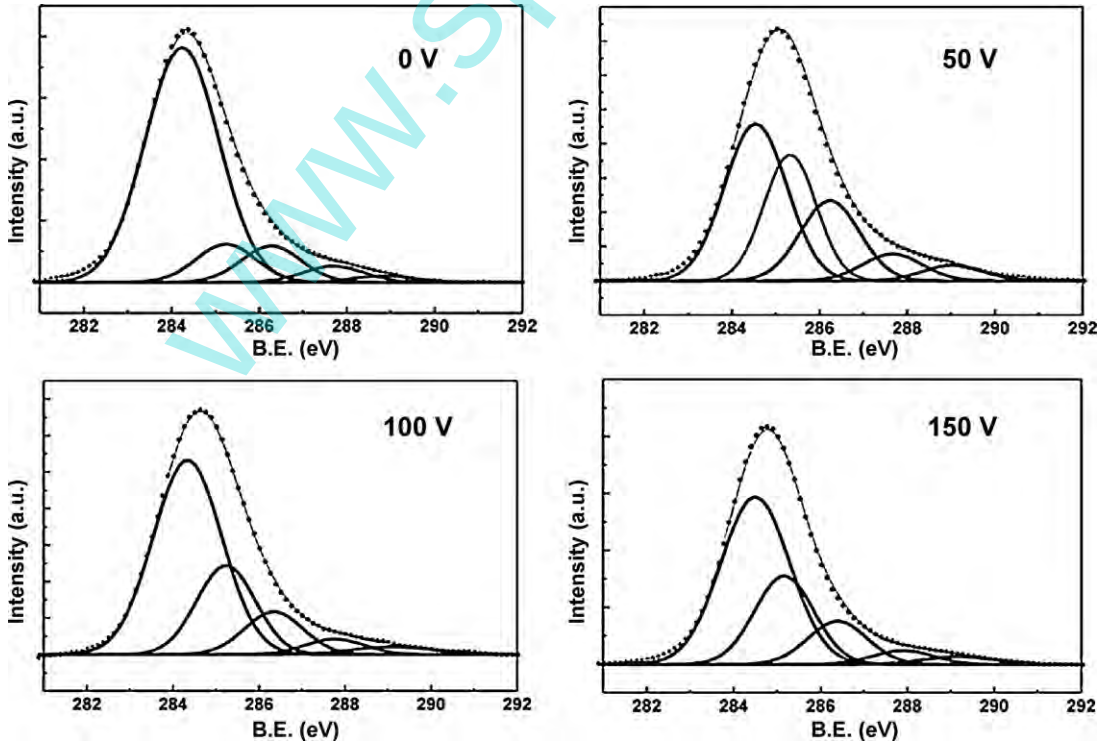

Fig. 3. XPS C1s core spectra of the CNx films deposited at different negative bias.

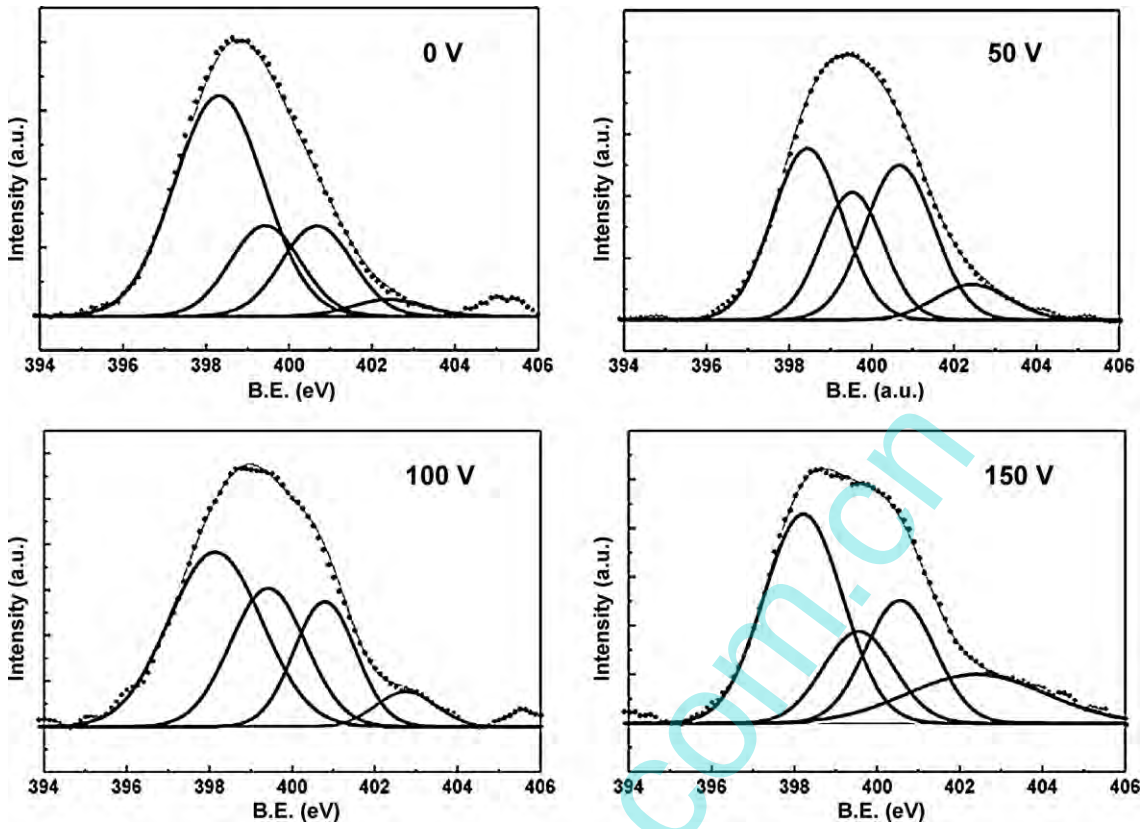

Fig. 4. XPS N1s core spectra of the CNx films deposited at different negative bias.

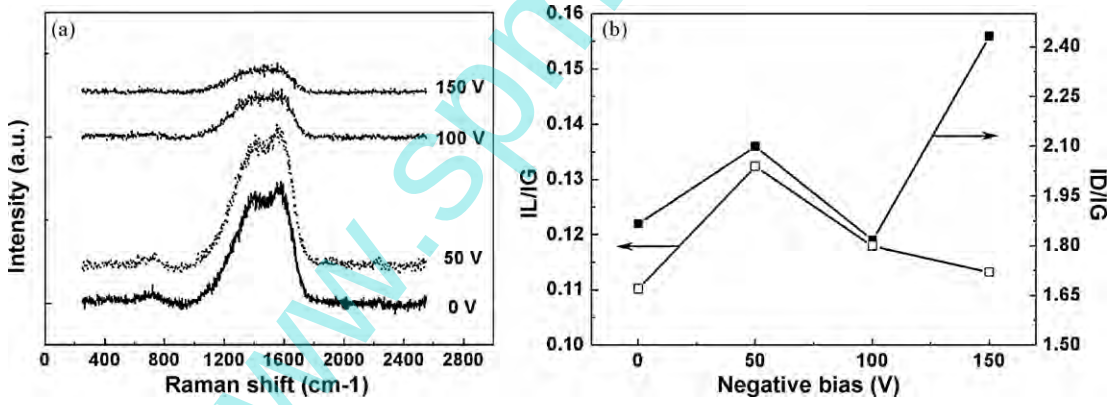

Fig. 5. The Raman spectra of the CNx films at different negative bias (a). I_D/I_G and I_L/I_G variation with the negative bias (b).

ture gives more specific surface area could adsorb mere oxygen atoms.

Raman spectra of the films in this study are shown in Fig. 5a. All the spectra showed broad band between 900 and 1800 cm^{-1}, with two main distinct contributions that a G peak originated from optical zone center vibrations (E_{2g} mode) of all pairs of sp^2 C atoms in aromatic rings and olefinic chains and a D shoulder peak originated from the breathing modes of sp^2 atoms in clusters of sixfold aromatic rings, respectively [20,21]. Other two peaks at about 700 and 2200 cm^{-1} can be ascribed to the presence of nitrogen, in particular to the out-of-plane transverse optic phonon near the M point zone boundary caused by the curvature of graphene planes induced by the incorporation of nitrogen, and to the C≡N bond, respectively [16,17].

Table 2
XPS N1s fitting results of the CNx films deposited at different negative bias.

Samples	N1	N2	N3	N4
0 V	58.0	19.3	19.0	3.7
50 V	35.0	25.0	32.5	7.5
100 V	43.5	28.5	21.8	6.2
150 V	43.4	17.4	22.5	16.7

To get a deep insight into the applied negative bias effect on the structure evolution of the CNx films, the Raman spectra between 900–1800 cm^{-1} and near 700 cm^{-1} (L peak) were all deconvoluted into Gauss peaks. The I_D/I_G ratio was the indicative of the cluster size and the degree of order in the clustered aromatic sp^2 phase of carbon films [22–25]. I_L/I_G was identified as the quantity of the curvature of graphene planes in this study. Fig. 5b gives the I_L/I_G and I_D/I_G variation with the negative bias. With the increasing of negative bias, both I_L/I_G and I_D/I_G increased at 50 V and decreased at the

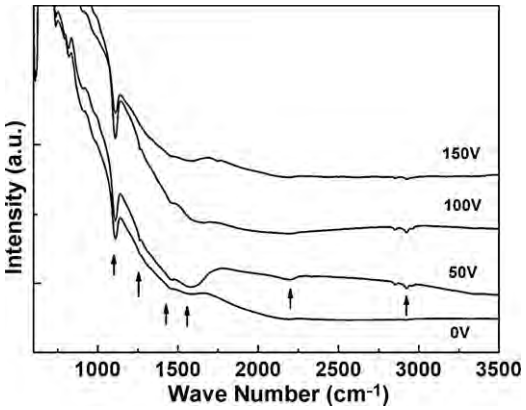

Fig. 6. FTIR spectra of the CNx films at different negative bias.

negative of 100 V. However, at the negative bias of 150 V, I_L/I_G and I_D/I_G gives different changes that the former decreased while the latter raised a little. G peak position reflects the bonding strength, and large full width at half maximum (Γ_G) reflects bond length and angle distortion [22–25]. In present work, the G peak positions and Γ_G had no obviously change (at about 1590 and 120 cm^{-1}, respectively) until the negative bias of 150 V was employed (at 1575 and 140 cm^{-1}). Thus, I_D/I_G increased at 50 V indicates a increasing of cluster size.

Fig. 6 shows the FTIR spectra in the range of 3500–750 cm^{-1} of a series of carbon nitride films deposited at the discharge voltages of 0, 50, 100, and 150 V. A broad absorption band between 1000 and 1700 cm^{-1} appeared in all the spectra. The appearance of this band in the FTIR spectra is the strongest evidence for the chemical incorporation of nitrogen atoms into the amorphous carbon network. After closer inspection of the FTIR spectra in this range, four peaks centered at 1100, 1253, 1380, and 1570 cm^{-1} could be clearly distinguished from the spectra. The peak of 1100 cm^{-1} was assigned to Si–O vibration and the others was attributed to the possible C=C, C=N, and C=N bonds [21,24,26]. A small peak at 2200 cm^{-1} was also observed obviously in the case of negative bias of 50 V, which may be attributed to the C≡N. The highest peaks at 1380, 1570 and 2200 cm^{-1} of the sample at 50 V implies that the nitrogen incorporation content achieved to the maximum, which was in good agreement with XPS and Raman results. The features in the spectral range 2800–3000 cm^{-1}, aroused from C–H stretching vibration.

3.3. Surface morphology

The surface morphology of the samples is characterized by AFM. For each sample, the same scan area (1 μm × 1 μm) was chosen in all measurements. Fig. 7 shows the AFM images obtained from the films deposited at 0 and 100 V. It is found from Fig. 7 that the surface of the film deposited at 0 V is rougher than that of the film deposited at 100 V. But we found that there is no simple relationship between the negative bias and the roughness of the films surfaces. The values of root mean square (RMS) roughness of the films with increasing the negative bias are 0.80, 1.10, 0.36 and 0.75, respectively. The trend of surface roughness of the films with the negative bias is in good agreement with the results of FE-SEM and Raman discussed above.

3.4. Field emission properties

The dependency of the emission current on the applied bias was measured by linearly increasing the voltage across the vacuum gap, and the resulted curves are shown in Fig. 8. With the increasing of the negative bias, the values of electric field required to obtain the

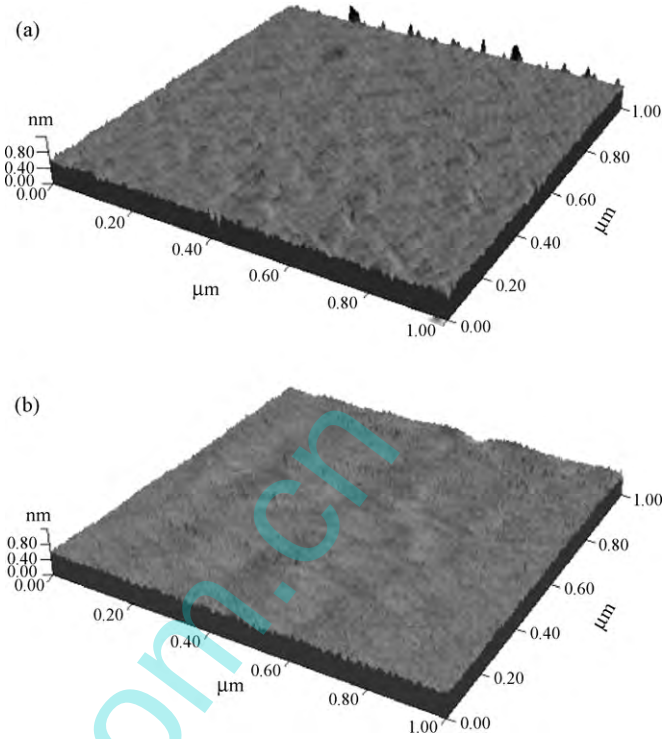

Fig. 7. The surface morphology of the as-deposited films: for the film deposited 0 V (a) and 100 V (b).

current density of 1 μA/cm^2 are 3.2, 4.0, 13.0 and 4.8 V/μm, and to obtain the current density of 10 μA/cm^2 are 13.5, 11.0, 22.5 and 14.5 V/μm, respectively.

It is well known that the incorporation of nitrogen atoms into carbon atoms acts as a weak donor state and alters the joint density of states in the films. Satyanarayana et al. [27] suggested that lower levels of nitrogen addition could increase emission significantly in a-C films. Zheng et al. proposed a model of bonding and band-forming [28], in which the involvement of nonbonding (lone pair) and lone-pair-induced antibonding (dipole) states is suggested to be responsible for lowering the work function and hence the electron emission threshold. That is to say, the nitrogen atoms state and joint density rather than nitrogen content plays the key role for lowering the threshold electric field of emitters in cold cathode emission. On the other hand, Carey et al. suggested that the size and concentration of sp^2 C clusters [29] play the key factors. The application of the external field will result in local field enhancement around the clusters and will aid in the emission of electrons.

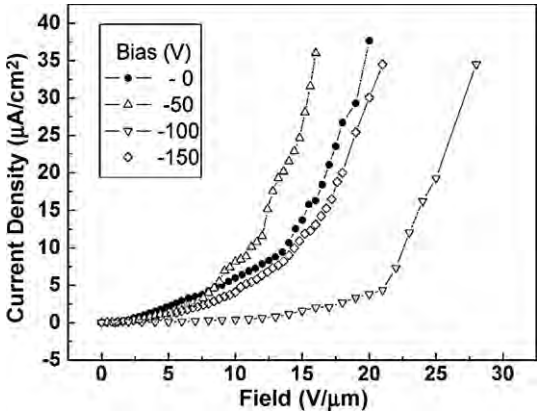

Fig. 8. Field emission properties for films deposited at different negative bias.

A similar conclusion was stated by Ilie et al. [30,31]. Besides, they concluded that sp^2 phase ordering in graphitic planes perpendicular to the emission direction was found to be clearly unfavorable to emission and increasing the cluster size derived from Raman spectroscopy in the 1–10 nm range improves emission [26,33]. In our present work, the size of sp^2 aromatic clusters is in the range of 1.8–2.4 nm, according to the Tuinstra–Koenig (TK) relationship [30]. These rich sp^2 carbon clusters with good connectivity in the films act as conduction part of the amorphous network, which lead to degrading electron emission barriers and raising Fermi level to enhance electron emission [31–33]. The lowering the threshold electric field in our work could be explained by the model of bonding and band-forming. However, the electron emission seems to be strongly related to the surface roughness: rougher surface means that there are more dense protrusions in the film surface, which can geometrically promote the enhancement of the electric field [34].

4. Conclusion

A series of nanostructures CNx film were deposited by reactive magnetron sputtering. SEM, XPS, Raman and FTIR results identify each other and show that, with the increase of the negative bias from 0 to 150 V, the nanocolumn structure of the CNx film degraded and the porous structure appeared. Nitrogen here plays a role for the formation of CNx nuclei at 0 V, which can be considered as the "seeds" for the growth of the columnar structures. At the lower negative bias, the bombardment with a low-energy particles stream could effectively enhance surface mobility and consequently facilitate film growth. However, at high negative bias (150 V), bonds in the interface of the disturbance particles were probably unstable, and could be easily broken out by high-energy particles bombardment, giving rise to a porous structure. The results suggest that the regular nanocolumns only can growth below the negative bias of 50 V. Furthermore, a comparison study of the field emission properties show that the field emission properties of the CNx films were related with the introduction of the nitrogen atoms, the size and concentration of sp^2 C clusters and the surface roughness. The films with rougher surface have lower threshold field in the present work.

Acknowledgements

The project was supported by "863" program of Chinese Ministry of Science and Technology, with grant No. 2007AA03Z338, and Technology of China and National Natural Science Foundation of China (Nos. 50823008, 50975273).

References

[1] J.J. Wang, M.Y. Zhu, R.A. Outlaw, X. Zhao, D.M. Manos, B.C. Holloway, Free-standing subnanometer graphite sheets, Appl. Phys. Lett. 85 (2004) 1265.
[2] L. Diederich, E. Barborini, P. Piseri, A. Podesta, P. Milani, A. Schneuwly, R. Gallay, Supercapacitors based on nanostructured carbon electrodes grown by cluster-beam deposition, Appl. Phys. Lett. 75 (1999) 2662.
[3] M.J. Colgan, M.J. Brett, Field emission from carbon and silicon films with pillar microstructure, Thin Solid Films 389 (2001) 1–4.
[4] S.K. Tripathi, N. Shukla, S. Dhamodaran, V.N. Kulkarni, Substrate atom enriched carbon nanostructures fabricated by focused electron beam induced deposition, Nanotechnology 19 (2008) 205302.
[5] K. Suenaga, C. Colliex, N. Demoncy, A. Loiseau, H. Pascard, F. Willaime, Synthesis of nanoparticles and nanotubes with well-separated layers of boron nitride and carbon, Science 278 (1997) 653–655.
[6] A.M. Morales, C.M. Lieber, A laser ablation method for the synthesis of crystalline semiconductor nanowires, Science 279 (1998) 208–211.
[7] K.Y. Lee, T. Ikuno, K. Tsuji, S. Ohkura, S. Honda, M. Katayama, K. Oura, T. Hirao, Synthesis of aligned bamboo-like carbon nanotubes using radio frequency magnetron sputtering, J. Vac. Sci. Technol. B 21 (2003) 1437–1441.
[8] S. Scalese, V. Scuderi, V. Privitera, A. Pennisi, F. Simone, Simultaneous catalyst deposition and growth of aligned carbon nanotubes on SiO_2/Si substrates by radio frequency magnetron sputtering, J. Appl. Phys. 102 (2007) 114905.
[9] X.W. Liu, J.H. Lin, W.J. Hsieh, H.C. Shih, The effect of pressure control on a thermally stable a-C:N thin film with low dielectric constant by electron cyclotron resonance-plasma, Thin Solid Films 409 (2002) 178–184.
[10] J. Lee, J. Kim, T. Hyeon, Recent progress in the synthesis of porous carbon materials, Adv. Mater. 18 (2006) 2073–2094.
[11] B. Zhang, Y. Yu, J. Zhang, Magnetron sputtering deposition of carbon nitride nanocolumns at low temperature, J. Phys. D: Appl. Phys. 42 (2009) 185304.
[12] S. Scalese, V. Scuderi, F. Simone, A. Pennisi, G. Compagnini, V. Privitera, Growth of aligned CNx nanocolumns on silicon by RF-magnetron sputtering, Carbon 44 (2006) 3123–3126.
[13] T. Inoue, S. Ohshio, H. Saitoh, K. Kamata, Preparation of nitrogen containing carbon films using chemical vapor deposition enhanced by electron cyclotron resonance plasma, Appl. Phys. Lett. 67 (1995) 353.
[14] H. Ling, J.D. Wu, J. Sun, W. Shi, Z.F. Ying, N. Xu, W.J. Pan, X.M. Ding, Z.Y. Zhou, Electron cyclotron resonance plasma-assisted pulsed laser deposition of boron carbon nitride films, Diamond Relat. Mater. 11 (2002) 1623–1628.
[15] N. Hellgren, M.P. Johansson, E. Broitman, P. Sandström, L. Hultman, J.-E. Sundgren, Effect of chemical sputtering on the growth and structural evolution of magnetron sputtered CNx thin films, Thin Solid Films 382 (2001) 146–152.
[16] S. Bhattacharyya, C. Cardinaud, G. Turban, Spectroscopic determination of the structure of amorphous nitrogenated carbon films, J. Appl. Phys. 83 (1998) 4491.
[17] S. Bhattacharyya, J. Hong, G. Turban, Determination of the structure of amorphous nitrogenated carbon films by combined Raman and X-ray photoemission spectroscopy, J. Appl. Phys. 83 (1998) 3917.
[18] H.-S. Jung, H.-H. Park, Micro-structural analysis of carbon nitride (CNx) film prepared by ion beam assisted magnetron sputtering, Diamond Relat. Mater. 11 (2002) 1205–1209.
[19] F.L. Normand, J. Hommet, T. Szörényi, C. Fuchs, E. Fogarassy, XPS study of pulsed laser deposited CNx films, Phys. Rev. B 64 (2001) 235416.
[20] A.C. Ferrari, J. Robertson, Interpretation of Raman spectra of disordered and amorphous carbon, Phys. Rev. B 61 (2000) 14095.
[21] C. Thomsen, S. Reich, Double resonant Raman scattering in graphite, Phys. Rev. Lett. 85 (2000) 5214.
[22] A.C. Ferrari, S.E. Rodil, J. Robertson, Interpretation of infrared and Raman spectra of amorphous carbon nitrides, Phys. Rev. B 67 (2003) 155306.
[23] G. Abrasonis, R. Gago, M. Vinnichenko, U. Kreissig, A. Kolitsch, W. Möller, Sixfold ring clustering in sp^2-dominated carbon and carbon nitride thin films: a Raman spectroscopy study, Phys. Rev. B 73 (2006) 125427.
[24] S.E. Rodil, A.C. Ferrari, J. Robertson, S. Muhl, Infrared spectra of carbon nitride films, Thin Solid Films 420 (2002) 122–131.
[25] S. Prawar, Y. Lifshitz, G.D. Lampert, E. Grossman, J. Kulik, I. Avigal, R. Kalish, Systematic variation of the Raman spectra of DLC films as a function of sp^2:sp^3 composition, Diamond Relat. Mater. 5 (1996) 433–438.
[26] I. Montero, L. Galán, O. Najmi, J.M. Albella, Disorder-induced vibration-mode coupling in SiO_2 films observed under normal-incidence infrared radiation, Phys. Rev. B 50 (1994) 4881.
[27] B.S. Satyanarayana, A. Hant, W.I. Miline, J. Robertson, Field emission from tetrahedral amorphous carbon, Appl. Phys. Lett. 71 (1997) 1430.
[28] W.T. Zheng, J.J. Li, X. Wang, X.T. Li, Z.S. Jin, B.K. Tay, C.Q. Sun, Electron emission of carbon nitride films and mechanism for the nitrogen-lowered threshold in cold cathode, J. Appl. Phys. 4 (2003) 2741.
[29] J.D. Carey, R.D. Forrest, R.U.A. Khan, S.R.P. Silva, Influence of sp^2 clusters on the field emission properties of amorphous carbon thin films, Appl. Phys. Lett. 77 (2000) 2006.
[30] F. Tuinstra, J.L. Koenig, Raman spectrum of graphite, J. Chem. Phys. 53 (1970) 1126.
[31] A. Ilie, A.C. Ferrari, T. Yagi, J. Robertson, Effect of sp-phase nanostructure on field emission from amorphous carbons, Appl. Phys. Lett. 76 (2000) 2627.
[32] J.J. Li, W.T. Zheng, Z.S. Jin, X. Wang, H.J. Bian, G.R. Gu, Y.N. Zhao, S.H. Meng, X.D. He, J.C. Han, Electron field emission of radio frequency magnetron sputtered CNx films annealed at different temperatures, J. Vac. Sci. Technol. B 21 (2003) 2382–2387.
[33] A. Ilie, A.C. Ferrari, T. Yagi, S.E. Rodil, J. Robertson, E. Barborini, P. Milani, Role of sp phase in field emission from nanostructured carbons, J. Appl. Phys. 90 (2001) 2024.
[34] J.J. Li, C.Z. Gu, P. Xu, Q. Wang, W.T. Zheng, Field emission enhancement of carbon nitride films by annealing with different durations, Mater. Sci. Eng. B 126 (2006) 74–79.